ANALYSIS ON STATIC RIGIDITY OF 6-UPS SURGICAL PARALLEL ROBOT FOR BONE FORMING

Heqiang Tian[1], Jiakun Jiang[1], Zhiqiang Dong[2], Chunjian Su[1]

ABSTRACT: Parallel robots have now been used for bone forming in orthopaedic surgeries widely, because of its high rigidity. The data mapping relation between robotic driving force and moving platform was obtained by Jacobin matrix and force equilibrium equation of robot, and then static rigidity matrix and static rigidity performance index of robot was further deduced by utilizing the virtual work principle. Then, rigidity property of the parallel robot under the unit force helix in a single direction was analysed, and the index of static rigidity performance was employed to analyse rigidity properties of the robot at the four fixed grinding postures. The results indicated that the parallel robot had the maximum composite rigidity at the centre, and the rigidity decreased with the distance from centre, which can meet the requirement of cervical vertebra grinding in the narrow operation space.

KEY WORDS: Orthopedic surgeries; Parallel robot; Bone forming; Static rigidity; Rigidity property

1 INTRODUCTION

In the field of biomedical engineering, especially for orthopedic surgery, a robot has become major manufacture machinery. By the use of the flexibility and automation of a robot, the bone forming in orthopedic surgeries can be finished accurately. A parallel robot, with compact structure, light weight and high rigidity, can be installed in the body of a patient directly so as to increase precision and safety of an operation, and hence is suitable for osteoplasty [1]. In recent years some special miniature parallel robots for orthopedic surgeries have been developed. Helmholtz Institute in Germany and TIMC Laboratory cooperated to carry out a project named as GRIGOS (Compact Robot for Image-Guided Orthopedic Surgery), in which a parallel robot with Stewart configuration was adopted in orthopedic surgeries [2]. SpineAssist Microrobot [3] special for spine surgeries adopts a parallel structure so as to make the volume of a mechanical structure decrease significantly. Korea Advanced Institute of Science and Technology (KAIST) developed an Arthrobot system based on Stewart parallel mechanism [4], which is mainly suitable for total hip arthroplasty (THA). Carnegie Mellon University developed a MBARS (Mini-Bone-Attached Robotics System) parallel robot system, which is used for patellofemoral arthroplasty (PFA).

[1] College of Mechanical and Electronic Engineering, Shandong University of Science and Technology, Qingdao 266590, China

[2] West coast (Development) Group Co., Ltd of Qingdao, Qingdao 266590, China

Surgical Orthdoc [6] and OrthoRoby robotic system [7] utilizes a parallel robot for bone grinding in an orthopedic surgery. Kim et al [8] used Cartesian parallel manipulator (CPM) for a total knee replacement. Stefano et al [9] adopted a robot with a parallel-series combined structure for total knee arthroreplasty (TKA), whose machined head is a parallel structure. Song et al [10] from Johns Hopkins University developed HyBar, an orthopedic parallel-series combined robot, which may be used for arthroplasty. Robotic Research Institute of Harbin Institute of Technology developed an orthopedic robot system based on X-ray image navigation [11], which can imitate the traditional treatment manipulation maneuver in long bone fracture reduction to perform reduction of the fractured bone. Finally, static rigidity performance of the robot during grinding of the cervical vertebra in an operation of cervical intervertebral replacement was evaluated.

For artificial cervical intervertebral disc replacement, the 6-UPS parallel robot system based on the Stewart platform was designed for grinding of the mating surface of an implanted prosthesis [12]. Static rigidity is a performance index critical for consideration of parallel robot use in a surgery. High rigidity can ensure less robot deformation during grinding of the cervical vertebra, so as to obtain higher positioning precision and increase precision of bone grinding. In this paper, firstly Jacobi matrix of the 6-UPS surgical parallel robot was established through vector construction. On this basis, the force equilibrium equation and static rigidity of the branched chain were established by utilizing the

helix theory, and afterwards static rigidity matrix of this type of robots was deduced by using the virtual work principle. Furthermore, rigidity performance of the parallel robot under the unit force helix in a single direction was discussed, and static rigidity of the robot under four fixed postures in bone grinding was analyzed.

2 MATERIALS AND METHODOLOGY

2.1 Structural composition of a parallel robot

Fulfillment of grinding of the cervical vertebra during cervical intervertebral disc replacement with a robot firstly requires that a robot should have enough freedom. In addition, the robot should have compact structure, small volume and light weight, and also possess the ability to adjust postures flexibly. Usually, a parallel mechanism is very suitable for grinding of the cervical vertebra in an operation of artificial cervical intervertebral disc replacement. By analyzing the operational procedure of artificial cervical intervertebral disc replacement, comparing current parallel mechanisms of 6-degree freedom, the Stewart type parallel robot was used as a mechanism for grinding the cervical vertebra, due to its big force, good rigidity, appropriate working space, small shape and stable motion. The upper platform of the mechanism adopted spherical hinge joints; the lower platform, Hooke hinge joints; and the drive shafts, a linear driving mechanism of ball screw-nut pairs with the maximum shaft length range at a minimal shaft length. That is to say, the mechanism is a Steward platform of 6-UPS configuration. Its structural and mechanical schematic diagrams were shown in Fig. 1.

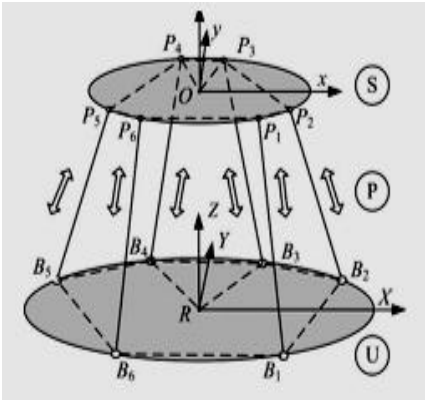

Fig.1 Structural and mechanical schematic diagrams of 6-UPS parallel robot.

2.2 Establishment of Jacobi matrix

Jacobi matrix of a parallel mechanism refers to differential relationship between a driving system and terminal position input and output, and plays an important role in a study on kinematics of a parallel mechanism. It is associated only with the kinematic size and driving link position, and reflects the status of a mechanical configuration. In this paper Jacobi matrix of the 6-UPS surgical parallel robot was solved by vector construction method [13].

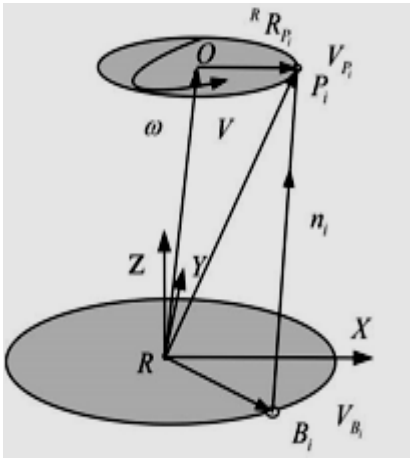

Fig.2 Velocity projection method.

As shown in Fig. 2, the motion of a rigid body may be decomposed into translational motion of a translational base point and rotation of a rotating base point. By choosing one motion branch of a parallel robot as an analytical object, the motion velocity of a hinge joint of the robot moving platform may be expressed as the following equation:

$$V_{P_i} = V + \omega \times {}^{R}R_{P_i} \tag{1}$$

where,

V_{P_i} — Velocity of the moving platform hinge P_i;

V — Velocity of the moving platform;

ω — Instantaneous angle velocity of the rotating base point O on the moving platform;

${}^{R}R_{P_i}$ — Description in the coordinate system $\{R\}$ of the vector from the base point O to the hinge P_i on the moving platform.

According the velocity projection principle, if velocity of the hinge P_i is projected to the vector n_i, the velocity of a branched shaft $\dot{l}_i$ should be equal to the projection velocity. The vector n_i may be determined by the hinge point P_i and B_i, i.e. ${}^{R}n_i = {}^{R}P_i - {}^{R}B_i$, and hence the following projection relation may be further obtained:

$$\dot{l}_i = V_{P_i}\,{}^{R}n_i \tag{2}$$

If the equation (1) is substituted in the equation (2), the following equation will be obtained:

$$\dot{l}_i = (V + \omega \times {}^R R_{P_i})\,{}^R n_i = [{}^R n_i^{\mathrm{T}}, ({}^R R_{P_i} \times {}^R n_i)^{\mathrm{T}}] \begin{bmatrix} V \\ \omega \end{bmatrix} \quad (3)$$

I.e.:

$$\begin{bmatrix} \dot{l}_1 \\ \dot{l}_2 \\ \vdots \\ \dot{l}_6 \end{bmatrix} = \begin{bmatrix} {}^R n_1^{\mathrm{T}}, ({}^R R_{P_1} \times {}^R n_1)^{\mathrm{T}} \\ {}^R n_2^{\mathrm{T}}, ({}^R R_{P_1} \times {}^R n_2)^{\mathrm{T}} \\ \vdots \\ {}^R n_6^{\mathrm{T}}, ({}^R R_{P_1} \times {}^R n_6)^{\mathrm{T}} \end{bmatrix} \begin{bmatrix} V \\ \omega \end{bmatrix} \quad (4)$$

And the equation above can be written for:

$$\begin{bmatrix} V \\ \omega \end{bmatrix} = J \begin{bmatrix} \dot{l}_1 \\ \dot{l}_2 \\ \vdots \\ \dot{l}_6 \end{bmatrix} \quad (5)$$

Where matrix J is:

$$J = \begin{bmatrix} {}^R n_1^{\mathrm{T}}, ({}^R R_{P_1} \times {}^R n_1)^{\mathrm{T}} \\ {}^R n_2^{\mathrm{T}}, ({}^R R_{P_1} \times {}^R n_2)^{\mathrm{T}} \\ \vdots \\ {}^R n_6^{\mathrm{T}}, ({}^R R_{P_1} \times {}^R n_6)^{\mathrm{T}} \end{bmatrix}^{-1} \quad (6)$$

Where ${}^R n_i = {}^R P_i - {}^R B_i$, ${}^R R_{Pi} = {}^R P_i - {}^R O$.

The matrix J represents a first order matrix of influence coefficients on posture outputting velocity versus posture inputting velocity in the robot, i.e. Jacobi matrix.

2.3 Establishment of static rigidity performance index

During a robot-assisted operation of cervical intervertebral disc replacement, a robot performed low speed and micro grinding in a narrow space. In this motion procedure, dynamic effect of the robot may be neglected, and then its rigidity performance in the operational workspace was evaluated by analyzing static rigidity of the parallel robot. Since the surgical parallel robot is assembled by many components in various link ways and motion ways, its deformation under the strain is most complex, and related to elastic deformation, plastic deformation, gap and friction. In order to simplify calculation, the following assumptions were made:

1) The deformation resulting from gravities of various components of the robot was minimal, and may be neglected.

2) The fixed platform, the moving platform and the linking hinges were rigid.

3) Various branched shafts of the robot deforms only along the axis of the branched shaft.

Based on the above assumptions, by analyzing and computing the degrees of position and posture deformation at the reference points on the moving platform of the parallel robot under external forces, its resistance on deformation was studied.

2.3.1 Establishment of static equation

When the posture of the 6-UPS surgical parallel robot is defined, the length values of 6 drive shafts of the robot $(l_1 \;\; l_2 \;\; l_3 \;\; l_4 \;\; l_5 \;\; l_6)$ will be defined; when the lengths of the 6 shafts are constant, the mechanism will become a stable one. If 6 force vectors are forced on the platform, the 6 shafts will generate reacting forces. As the main stress forces of the shaft are along the shaft axis, i.e. other forced may be neglected, these reacting forces will generated along the shaft axis. When 6 axis forces are expressed as force screw to consider balance of the moving platform, the sum of force screw of the 6 shafts should keep balance with 6 dimensional force of the moving platform. And hence, the force equilibrium equations were established according to the helix theory in a way as described in reference [14].

As shown in Fig. 3, in the moving coordinate system $\{O\}$, the position vectors of 6 hinge points P_i on the moving platform is expressed as ${}^O P_i$; in the fixed coordinate system $\{R\}$, the position vectors of 6 hinge points P_i on the moving platform as ${}^R P_i$; in the fixed coordinate system $\{R\}$, the position vectors of 6 hinge points P_i on the fixed platform as ${}^R B_i$, where $i = 1, 2, \cdots, 6$. Given that F and M represent the principal vector and the principal moment of forces against the moving platform versus the coordinate origin respectively, f_i represents the driving force along the ith branched shaft, s_i the unit vector of the axis of the ith branched shaft versus the coordinate system, and ${}^R R_{Pi}$ description in the coordinate system $\{R\}$ of the vector form the moving platform origin to the moving platform hinge P_i, where $i = 1, 2, \cdots, 6$, the static equation of the moving platform of the parallel robot versus the defined coordinate system $\{R\}$ may be obtained as follows:

$$f_1 s_1 + f_2 s_2 + \cdots + f_6 s_6 = F \quad (7)$$

$${}^R R_{P1} \times (f_1 s_{01}) + \cdots + {}^R R_{P6} \times (f_6 s_{06}) = M \quad (8)$$

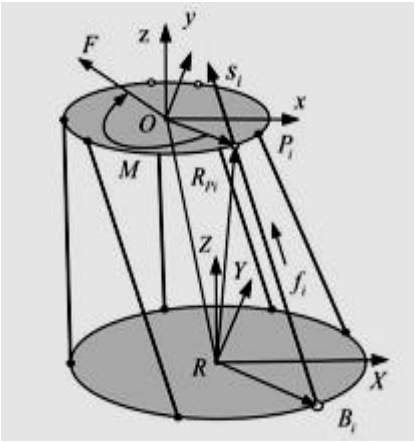

Fig.3 Analysis on stress forces of 6-UPS surgical parallel robot.

The above static equation may be modified as a matrix equation as follows:

$$\begin{bmatrix} F \\ M \end{bmatrix} = Gf \tag{9}$$

Where G is the first order matrix of influence coefficients, which is also called Jacobin matrix:

$$G = \begin{bmatrix} s_1 & s_2 & s_3 & s_4 & s_5 & s_6 \\ s_{01} & s_{02} & s_{03} & s_{04} & s_{05} & s_{06} \end{bmatrix} \tag{10}$$

Where

$$s_i = \frac{{}^R P_i - {}^R B_i}{\left| {}^R P_i - {}^R B_i \right|} \tag{11}$$

$$s_{0i} = {}^R R_{Pi} \times s_i \tag{12}$$

$${}^R R_{Pi} = {}^R P_i - {}^R O \tag{13}$$

2.3.2 Static rigidity of branched chain

Each branched chain of a parallel mechanism adopts the driving mode of servo motor plus ball screw-nut, and rotation of servo motor may be transformed to linear motion of the moving pair driven by the nut. According to the third assumption mentioned above, if other deformations of various branched shafts of the surgical parallel robot are not considered, compression deformations will occur only along the axis of the ball screw shaft. Given that one linear branched shaft of parallel robot with variable shaft length generates the elastic deformation Δl_i under the driving force f_i; the following equation will be obtained:

$$f_i = k_i \Delta l_i \tag{14}$$

Where k_i represents rigidity coefficient of each branched shaft, which is associated with the elastic modulus E of the branched shaft material and its cross section area A and length l_i:

$$k_i = \frac{EA}{l_i} \tag{15}$$

By considering stress deformation of the six branches, the rigidity of the six branched shafts is expressed as a matrix:

$$f = K\Delta l \tag{16}$$

Where

$f = \begin{pmatrix} f_1 & f_2 & f_3 & f_4 & f_5 & f_6 \end{pmatrix}^T$;

$K = \mathrm{diag}\begin{pmatrix} k_1 & k_2 & k_3 & k_4 & k_5 & k_6 \end{pmatrix}$;

f_i: driving force of the *i*th branched shaft;

k_i: rigidity of the *i*th branched shaft.

2.3.3 Matrix of static rigidity

When the configuration size and structural parameters of the surgical parallel robot are known, the matrix G may be obtained easily according the equation (10). In the case that the helix F of the 6-dimension forces is known, the rod-connecting force f may be solved, and when G is not singular, the following equation will be obtained:

$$f = G^{-1}F \tag{17}$$

Based the virtual work principle, Gosselin [15] established projection relationship between spatial mechanical manipulation force and terminal deformation. Given that Δl is the virtual displacement produced by the driving force f on the drafts, and ΔP is the virtual displacement produced by the external stress helix F on the terminal end of the moving platform, the algebraic sum of the work of the external stress applied unto the mechanism at its generated virtual displacement will be zero, i.e.:

$$F\Delta P - f\Delta l = 0 \tag{18}$$

The following equation may be obtained from the equation (5):

$$\Delta P = J\Delta l \tag{19}$$

Where Δl is the increment of rod length of the robot, $\Delta l = \begin{pmatrix} \Delta l_1 & \Delta l_2 & \Delta l_3 & \Delta l_4 & \Delta l_5 & \Delta l_6 \end{pmatrix}^T$, where $\Delta l_i \ (i = 1, 2, \ldots, 6)$ represents deformation of the ith branched rod of the robot and ΔP is the increment of the robot pose and position.

The equation (19) is substituted in the equation (20); the following equation will be obtained:

$$f = J^T F \tag{20}$$

The following equation may be obtained from the equation (17) and (20):

$$J^T = G^{-1} \tag{21}$$

It can be seen that Jacobin matrix of the parallel robot and the first order matrix of static influence coefficients are an inverse transposition matrix pair.

By integrating the equation (16), (19), (20) and (21), the equation of stress forces versus robot deformation may be obtained:

$$F = GKG^{\mathrm{T}}\Delta P \tag{22}$$

Therefore, the rigidity matrix D of the surgical parallel robot is:

$$D = GKG^{T} \tag{23}$$

Then

$$\Delta P = D^{-1}F \tag{24}$$

$$\left[\Delta x \quad \Delta y \quad \Delta z \quad \Delta\alpha \quad \Delta\beta \quad \Delta\gamma\right]^{T} = D^{-1}F \tag{25}$$

It is can be know form the equation (25), that the broadly-defined displacement in this direction generated by the parallel robot under the unit force helix in a single direction is the flexibility of the robot in this direction, i.e. the reciprocal of the rigidity in this direction. The equations are shown as follows:

$$\begin{cases} 1/k_x = \Delta x = D^{-1}(1,:)[1 \quad 0 \quad 0 \quad 0 \quad 0 \quad 0]^T \\ 1/k_y = \Delta y = D^{-1}(2,:)[0 \quad 1 \quad 0 \quad 0 \quad 0 \quad 0]^T \\ 1/k_z = \Delta z = D^{-1}(3,:)[0 \quad 0 \quad 1 \quad 0 \quad 0 \quad 0]^T \\ 1/k_\alpha = \Delta\alpha = D^{-1}(4,:)[0 \quad 0 \quad 0 \quad 1 \quad 0 \quad 0]^T \\ 1/k_\beta = \Delta\beta = C^{-1}(5,:)[0 \quad 0 \quad 0 \quad 0 \quad 1 \quad 0]^T \\ 1/k_\gamma = \Delta\gamma = C^{-1}(6,:)[0 \quad 0 \quad 0 \quad 0 \quad 0 \quad 1]^T \end{cases} \tag{26}$$

Where k_x、k_y、k_z、k_α、k_β、k_γ represent rigidities of the robot system along the axis x, y and z and those around the axis x, y and z; $D^{-1}(i,:)\ \ i = 1,2,...,6$ represent all the elements the row *i* of the flexibility matrix.

2.3.4 Index of static rigidity

Assuming that λ_i and A_i represent the characteristic values and the corresponding characteristic vectors of the rigidity matrix of one configuration in its workspace respectively, λ_i will represent the rigidity of the parallel robot in the direction of A_i.

The following equation may be obtained from the equation (22) and (23):

$$\Delta P = D^{-1}F \tag{27}$$

If the two norms of the equation (27) are chosen, the following equation may be obtained:

$$\left\|\Delta P\right\|_2 = F^{T}(D^{-1})^{T}D^{-1}F \tag{28}$$

From properties of the matrix norms, the following equation may be obtained:

$$\left\|\Delta P\right\|_2 = \left\|D^{-1}F\right\|_2 \le \left\|D^{-1}\right\|_2 \left\|F\right\|_2 \tag{29}$$

When *F* is known, the maximum of ΔP will be dependent on D^{-1}. By introducing the Lagrange multiplier λ, the following Lagrange function will be obtained:

$$L = F^{\mathrm{T}}(D^{-1})^{\mathrm{T}}D^{-1}F - \lambda(F^{\mathrm{T}}F - 1) \tag{30}$$

It can be obtained from necessary conditions of the relative limits that the Lagrange multiplier λ is the characteristic value of the matrix $(D^{-1})^{\mathrm{T}}D^{-1}$. Hence, $\left\|D^{-1}\right\|_2$ is the square root of the maximum characteristic value of the matrix $(D^{-1})^{T}D^{-1}$, i.e. the maximum characteristic value meets the equation $\left\|D^{-1}\right\|_2 = \sqrt{\lambda_{\max}}$, where $\lambda_{\max}$ is the maximum characteristic value of the matrix $(D^{-1})^{T}D^{-1}$. Given that $S = \sqrt{\lambda_{\max}}$ and $\left\|F\right\|_2 = 1$, then the following equation may be obtained:

$$\left\|\Delta P\right\|_2 \le S \tag{31}$$

Therefore, S may be used as the index of static rigidity performance to measure static rigidity of the parallel robot for grinding of the cervical vertebra. The smaller S, the weaker the robot deformation, higher the static rigidity, and on the contrary the lower the rigidity.

3 RESULTS

After structural parameters of a parallel mechanism are defined, their rigidities will vary with postures of the mechanism. From a viewpoint of mechanism design, the minimum rigidity of the parallel mechanism should be greater than the given value so as to ensure the mechanism precision in the workspace. The indices to evaluate rigidity of a parallel mechanism include path, determinant, condition number and characteristic value [16]. In this paper the square root S of the maximum of the rigidity matrix of a parallel mechanism was used as the evaluation index to investigate rigidity distribution of the robot in the given workspace.

3.1 Analysis on rigidity in a single dimension

At first, rigidity performances of the parallel robot along the axis x, y and z, and around the axis x, y and z under the unit force helix in a single dimension were analysed by utilizing the equation (26), as shown in Fig.4.

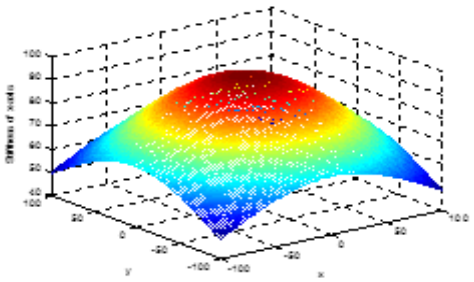

a) Along the axis x

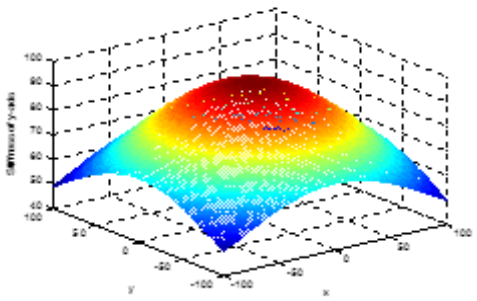

b) Along the axis y

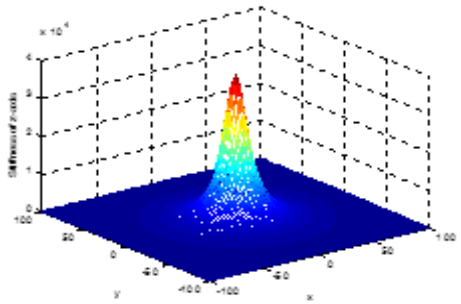

c) Along the axis z

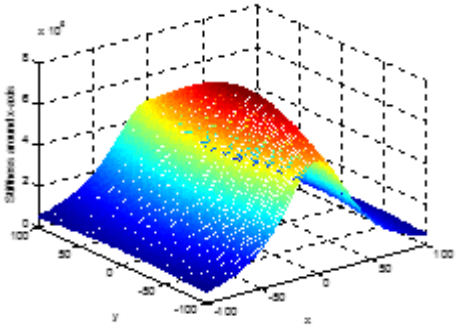

d) Around the axis x

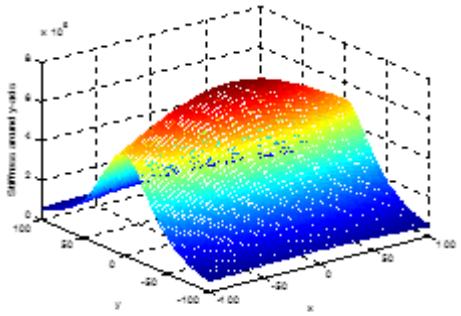

e) Around the axis y

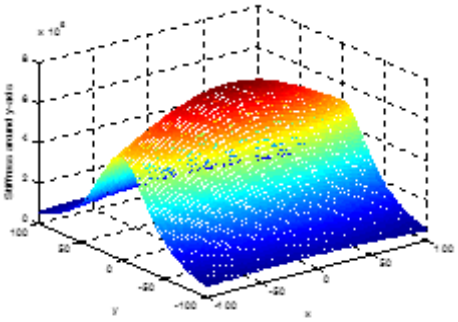

e) Around the axis y

Fig.4 Rigidity distribution of surgical parallel robot at each axis.

It can be seen from the figures of rigidity distribution of the surgical parallel robot at each axis, in the operational spaces of $-50mm \le x \le 50mm$ and $-50mm \le y \le 50m$, rigidities of the surgical parallel robot at each axis become greater near the centre on the XY plane, and decrease gradually with the distance from each axis. Among the changes, the rigidity change trend along the axis x agrees with that along the axis y and rigidity values increase gradually toward the axis centre, while rigidity values along the axis z increase sharply near the centre point of the axis. Rigidity values around the axis x increase stably toward the axis centre; those around the axis y increase rapidly toward the axis centre; and those around the axis z increase gradually toward the axis centre.

3.2 Analysis on composite static rigidity

Since during bone grinding postures of the robot are fixed, static rigidity has effect on positioning precision of a grinding tool. By analyzing working status of the robot during an operation, we utilized the static rigidity index S to analyze static rigidity distribution at the four postures $(x, y, 220, 0, 0, 0)$, $(x, y, 220, 10, 0, 0)$, $(x, y, 220, 0, 10, 0)$ and $(x, y, 220, 0, 0, 10)$ on the plane XY, and the results were shown in Fig.5.

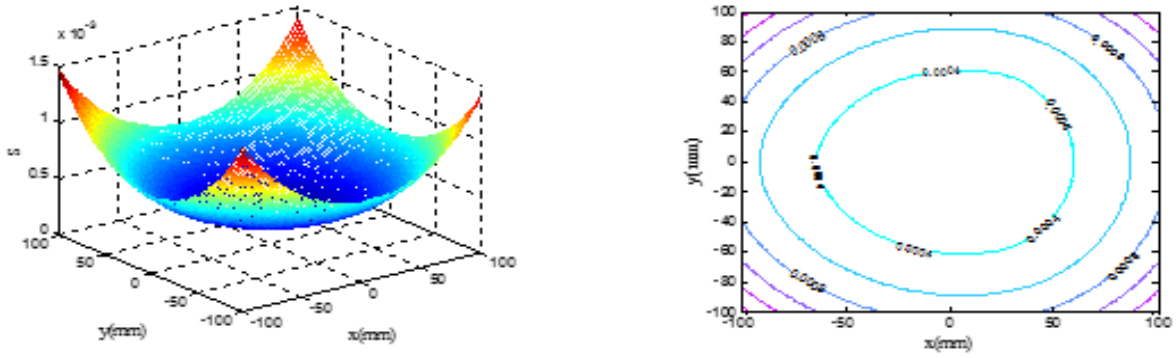

a) Position and pose $(x, y, 220, 0, 0, 0)$

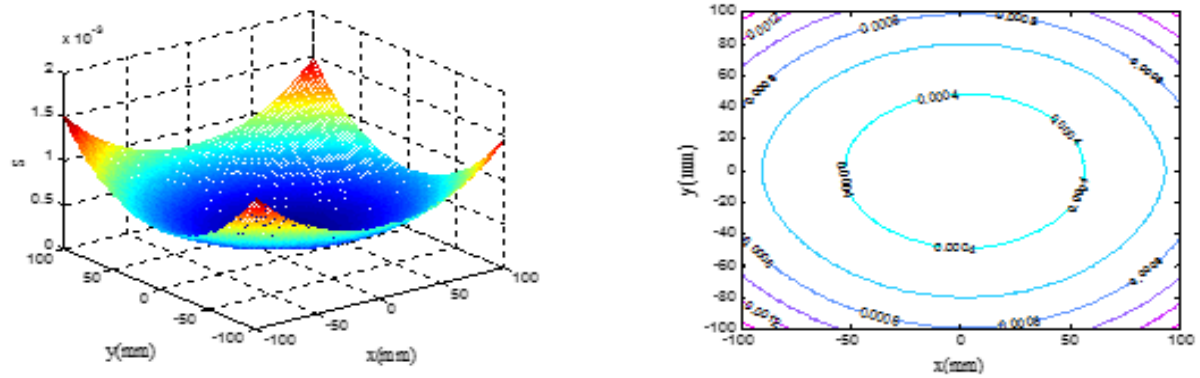

b) Position and pose $(x, y, 220, 10, 0, 0)$

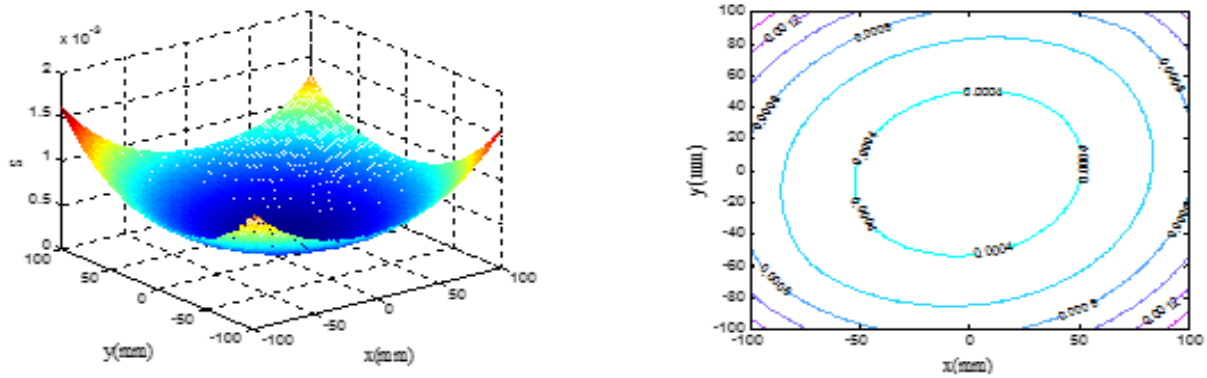

c) Position and pose $(x, y, 220, 0, 10, 0)$

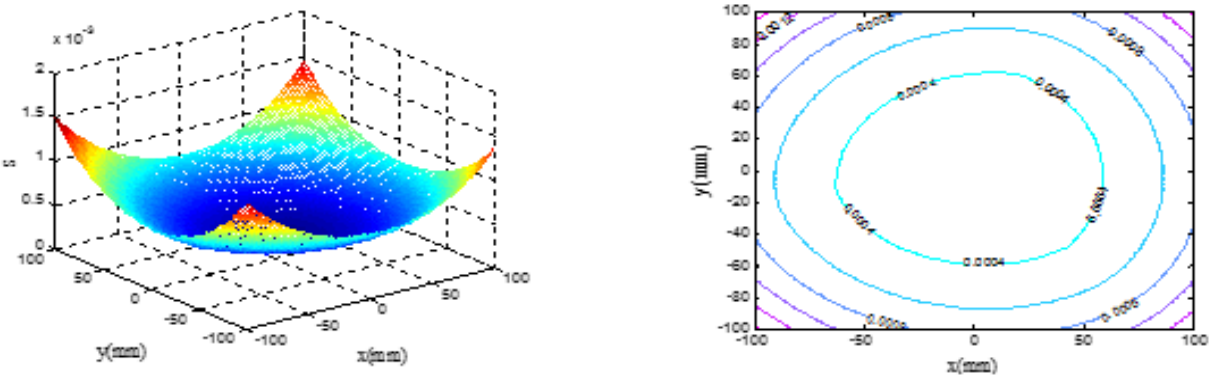

d) Position and pose $(x, y, 220, 0, 0, 10)$

Fig.5 Maximum deformation distribution of surgical parallel robot.

It can be seen from the figures of rigidity distribution of the surgical parallel robot at each axis, in the operational spaces of $-50mm \le x \le 50mm$ and $-50mm \le y \le 50mm$, rigidities of the surgical parallel robot at each axis become greater near the centre on the XY plane, and decrease gradually with the distance from each axis. Among the changes, the rigidity change trend along the axis x agrees with that along the axis y and rigidity values increase gradually toward the axis centre, while rigidity values along the axis z increase sharply near the centre point of the axis. Rigidity values around the axis x increase stably toward the axis centre; those around the axis y increase rapidly toward the axis centre; and those around the axis z increase gradually toward the axis centre.

4 CONCLUSION

1) The designed 6-UPS parallel robot has high rigidity and flexibility, and can enhance precision and safety of a surgery.

2) With vector construction method, Jacobin matrix of the 6-UPS parallel robot has been solved, the force balance equation has been established based on the helix theory and the static rigidity matrix and performance index have been deduced by using the virtual work principle.

3) Based on the above rigidity model, the rigidity performance of the parallel robot along and around the axis x, y and z under the unit force helix at one single dimension has been analyzed; and the rigidity performance properties of the robot at the four fixed postures have been analyzed by utilizing the static rigidity index S.

4) The analysis results indicate that the composite rigidity of the parallel robot has the maximum at the axis centre, and decreases with the distance from the centre, i.e. the robot has the optimal rigidity performance when working in the operation space near the body axis.

5 ACKNOWLEDGEMENTS

The authors would like to express appreciation to financial supports from Shandong Province Young and Middle-Aged Scientists Research Awards Fund (BS2013ZZ011), Qingdao application foundation research project (Youth special) (14-2-4-120-jch), Scientific Research Foundation of Shandong University of Science and Technology for Recruited Talents (2013RCJJ016), National Natural Science Foundation of China (51305241) and Shandong province high school scientific research plan project (J12LA03).

6 REFERENCES

► [1]P Cinquin, J Troccaz, J Demongeot, S Lavallee, G Champleboux, L Brunie, F Leitner, P Sautot, B Mazier, A Perez, M Djaid, T Fortin, M Chenic, A Chapel, "IGOR: Image guided operating robot", Innov.Technonogie Biologie Med., vol. 13, pp. 374-394, 2010.

► [2]Brandt G, Zimolong A, Carrat L, et al, "CRIGOS: a compact robot for image-guided orthopedic surgery", IEEE Trans Inf Technol Biomed, vol. 3, No.4, pp.252-260, 1999.

► [3]Pechlivanis I, Kiriyanthan G, Engelhardt M, Scholz M, Lücke S, Harders A, Schmieder K, "Percutaneous placement of pedicle screws in the lumbar spine using a bone mounted miniature robotic system: first experiences and accuracy of screw placement", Spine, vol.34,No.4, pp.392-398, 2009.

► [4]Kwon DS, Yoon YS, Lee JJ, Ko SY, Huh KH, Chung JH, Park YB, "ARTHROBOT: a new surgical robot system for total hip arthroplasty ", Proceedings of the IEEE/RSJ Int. Conf. Intelligent Robots and Systems, IEEE,pp.1123-1128, 2001.

► [5]Wolf a, Jaramaz B, Lisien B, et al, "MBARS: mini bone-attached robotic system for joint arthroplasty", International Journal of Medical Robotics and Computer Assisted Surgery, vol.1, No.2, pp.101-121, 2005.

► [6]Kwon DS, Lee JJ, Yoon YS, Ko SY, Kim J, Chung JH, Won CH, Kim JH, " The mechanism and the registration method of a surgical robot for hip arthroplasty", Proceedings of the 2002 IEEE International Conference on Robotics and Automation, IEEE, vol.2,pp.1889-1894,2002.

► [7]Barkana DE, "Design and implementation of a control architecture for a robot-assisted orthopedic surgery", Int. J. Med. Robot. Comp. Assist. Surg., vol.6, No.1, 42-56, 2010.

► [8]Kim HS, Tsai LW, "Design Optimization of a Cartesian Parallel Manipulator", Journal of Mechanical Design, vol.125, pp.43-51, 2003.

► [9]Stefano Bruni, Pietro Cerveri, Ivan Espinosa, "An Application of a Hybrid Robot in the Total Knee Replacement Procedure", The 12th IFToMM World Congress, Besançon, France, 2007.

► [10]S Song, A Mor, B Jaramaz, "HyBAR: Hybrid bone-attached robot for joint arthroplasty", Int. J. Med. Robot. Comp. Assist. Surg., vol.5, No.2, pp.223–231, 2009.

► [11]Sun lining, Zhang jian, Du zhijiang, Fu lixin, "A Fluoroscopy-Based Orthopedic System for Locking Intramedullary Nails", 3nd International Symposium on Instrumentation Science and Technology, vol.3, pp.621-625, 2004.
► [12]Heqiang Tian, Dongmei Wu, Zhijiang Du, Lining Sun, "Design and Analysis of a 6-DOF Parallel Robot Used in Artificial Cervical Disc Replacement Surgery", Proceedings of the 2010 IEEE International Conference on Information and Automation (ICIA), Harbin, pp.30-35, 2010:
► [13]Fan R, Liu H, Wang D, " Statics and stiffness of 3DOF parallel loading mechanism", Journal of Beijing University of Aeronautics & Astronautics, vol.40,No7,pp.861-866,2014.
► [14]Li Jia, Chen Ken, Dong Yi, et al, "Study on the static stiffness of the parallel flexure joint robot", Journal of Tsinghua University, vol.39, No.8, pp.16-20. 1999.
► [15]Gosselin C, "Stiffness mapping for parallel manipulators", Robotics & Automation IEEE Transactions on, vol.6, No.3, pp.377 – 382, 1990.
► [16]Rezaei A, Akbarzadeh A, Akbarzadeh-T. M R, "An investigation on stiffness of a 3-PSP spatial parallel mechanism with flexible moving platform using invariant form", Mechanism & Machine Theory, vol.51, No. 5, pp.195–216, 2012.